Journal of University of Science and Technology Beijing
Vol.7(2000), No.3, p.170

Metallurgy

Fluid Flow Behavior of Liquid in Cylindrical Vessels Stirred by One or Two Air Jets

Lifeng Zhang[1], *Shoji Taniguchi*[1], *Kaike Cai*[2], *Ying Qu*[2]

1) Department of Metallurgy Graduate School of Engineering, Tohoku University, Sendai 980-8579 Japan;
2) Metallurgy School, University of Science and Technology Beijing, Beijing 100083, China
(Received 1999-10-10)

Abstract: Based on the two-phase model (Eulerian-Eulerian model), the three dimensional fluid flow in water and that liquid steel systems stirred by one or two multiple gas jets are simulated. In the Eulerian-Eulerian two-phase model, the gas and the liquid phase are considered to be two different continuous fluids interacting with each other through the finite inter-phase areas. The exchange between the phases is represented by source terms in conversation equations. Turbulence is assumed to be a property of the liquid phase. A new turbulence modification k-ε model is introduced to consider the bubbles movement contribution to k and ε. The dispersion of phases due to turbulence is represented by introducing a diffusion term in mass conservation equation. The mathematical simulation agrees well with the experiment results. The study results indicate that the distance of two nozzles has big effect on fluid flow behavior in the vessel. Using two gas injection nozzles at the half radii of one diameter of the bottom generates a much better mixing than with one nozzle under the condition of the same total gas flow rate.

Key words: fluid flow; two-phase Eulerian-Eulerian model; model; mathematical simulation

1 Introduction

Gas-injection continues to play an increasing important role in metallurgical processing operations such as steelmaking, ladle metallurgy, ferroalloy production, and nonferrous extraction and refining. The effectiveness of gas injection in promoting gas-metal reactions and/or enhancing bath stirring in these processes is linked to the degree of dispersion of gas in the bath, the velocity of the gas in liquid phase, and the size of the bubbles. Extensive numerical modeling of various aspects of air-stirred refining operations has been carried out and reported [1–5], such as hydrodynamics, heat and mass transfer, turbulence phenomena and mixing phenomena, *etc*. However, the considerable body of this work mainly concerned with bottom-centered one nozzle injection case. In the industrial process, multiple gas jets have been used in some systems to improve the stirring condition, chemical reaction in bath or improve inclusion removal from bath [6]. Until now, only few papers on the case of multiple gas jets can be found [7, 8]. Miao-Yong Zhu *et al.* [7] mathematically studied the effect of gas injection mode on the fluid flow and the bath mixing for a water model of ladle systems, but did not make experiment to verify the mathematical simulation. Recently, K. Sasaki *et al.* [8] experimentally studied the gas hold-up distribution and the velocity distribution of gas phase and water phase in the cylindrical vessels stirred by one or two air jets, but no mathematical simulation. Therefore, it is useful to develop a model to predict the fluid flow of the gas-liquid system stirred by one or two gas jets, and make a comparison with the experiment results.

In this paper, based on a two-phase (Eulerian-Eulerian) model, the three dimensional fluid flow in the water systems stirred by one or two multiple gas jets is simulated. The effect of distance between the two injection nozzles on the fluid flow is discussed.

The objected system is the same as that of the experiment of K. Sasaki *et al.* [8](**figure 1**), here only a brief

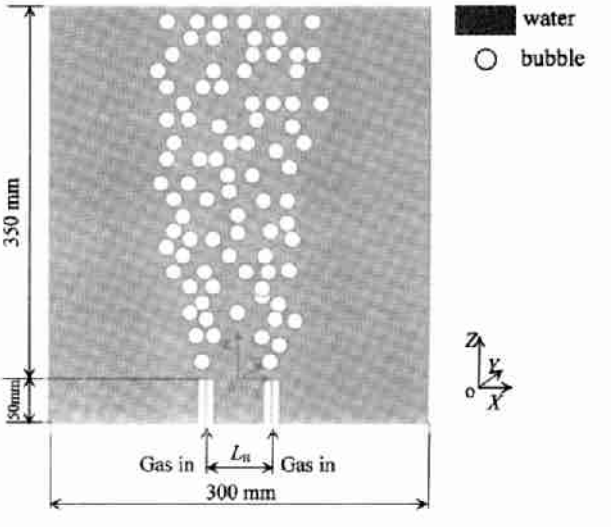

Figure 1 Schematic of the objected vessel.

outline is given. A glass vessel with a diameter of 300 mm and 350 mm height filled with water. Air gas is injected into water by one or two nozzles with a diameter of 2 mm. As for two nozzles, the gas flow rate of every one is 40×10^{-6} m^3/s, the location of the two nozzles is showed in figure 1, $L_H=20$ mm; as for only one nozzle, the outlet of this nozzle is located in the center of the bottom, the gas flow rate is 80×10^{-6} m^3/s. The coordinate configuration is showed in figure 1. The physical parameters of water and gas are as follows [9]: $\rho_{water}=1\,000$ kg/m^3, $\rho_{air}=1.29$ kg/m^3, $\mu_{water}=0.001$ Pa·s, $\sigma_{water}=0.073$ N/m.

2 Mathematical Formulation

In the Eulerian-Eulerian two-phase model, the gas and the liquid phase are considered to be two different continuous fields, which are separated by sharp (but flexible) boundaries. They are immiscible, interpenetrating and interacting with each other through the finite inter-phase areas. Mass conservation, momentum equations are derived for each phase considering the time averaged variables. The exchange between the phases is represented by the source terms in conversation equations. The phases are assumed to share space in proportion to their volume fractions so as to satisfy the total continuity relation, so

$$\alpha_1+\alpha_2=1 \tag{1}$$

Turbulence is assumed to be a property of the liquid phase, the pressure of gas phase is assumed to be the same that of liquid phase, *i.e.*, only one pressure is to be solved. Introducing a diffusion term into mass conservation equation represents the dispersion of the phases due to turbulence.

In the present study gas bubbles are rigid, spherical and with a uniform throughout size. Bubble coalescence and breakup are not taken into account, *i.e.*, bubble-bubble interactions are assumed to be negligible.

Thermal interaction is ignored, the entire system being assumed isothermal, and flow is essentially Newtonian, incompressible and steady.

2.1 Governing equations

Within the framework of the above assumption, the governing equations may be put in the following forms.
(1) Continuity equation for phase m.

$$\nabla\cdot(\alpha_m\rho_m U_m-D\nabla\alpha_m)=0 \tag{2}$$

The second term represents the phase diffusion term accounts for the turbulent dispersion of the bubbles due to turbulence in the continuous phase. D is effective phase diffusion (dispersion) coefficient to represent the random motion associated with the phases which is expressed as

$$D=\frac{\mu_t}{Pr} \tag{3}$$

where μ_t is the turbulent viscosity; Pr is the dispersion Prandtl number, in the present paper, the value of Pr takes 1 [1].

(2) Conservation of momentum for velocity of every phases.

$$\nabla\cdot(\alpha_m\rho_m U_m U_m-\alpha_m\Gamma_m\nabla U_m)=S_m+S_m^* \tag{4}$$

Convection Diffusion Source

Where, Γ_m is an exchange coefficient representing the effects of turbulent and/or laminar diffusion within the phases. The appropriate forms of these terms are given in **table 1**. k-ε two-equation model is applied to simulate turbulence. So, in table 1, the effective viscosity is

Table 1 Exchange cofficient and source terms

ϕ_m	Γ_m	S_m	S_m^*
$U_{1,i}$	μ_{eff}	$-\alpha_1\frac{\partial P}{\partial x_i}+\alpha_1\rho_1 g_i$	F_i
$U_{2,i}$	μ_{eff}	$-\alpha_2\frac{\partial P}{\partial x_i}+\alpha_2\rho_2 g_i$	$-F_i$
k	μ_t/σ_k	$\alpha_1\rho_1(G-\varepsilon)$	0
ε	μ_t/σ_ε	$\alpha_1\rho_1\frac{\varepsilon}{k}(C_1G-C_2\varepsilon)$	0

$$\mu_{eff}=\mu_t+\mu_l \tag{5}$$

where G is the volumetric rate of generation of k which can be expressed as:

$$G_k=\mu_{eff}\frac{\partial U_i}{\partial x_i}\left(\frac{\partial U_i}{\partial x_j}+\frac{\partial U_j}{\partial x_i}\right) \tag{6}$$

2.2 Some parameters

(1)Turbulence model.

Turbulence is assumed to be a property of the first phase, modeled transport equations for the turbulent kinetic energy k and its dissipation rate ε are solved only for this phase. The k–ε two-equation model, by far the most widely used two-equation eddy-viscosity turbulence model, is applied in the present study but modify this model in order to consider the bubbles movement contribution to the k and ε. There have been a number of proposals for exerting turbulence model to account for the additional production of turbulence due to the presence of bubbles. At present, the mainly used method is to insert volumetric source terms, which are associated with the migration of gas bubbles through the liquid are added into the standard k and ε equations

[1, 4].

In the present paper, another method, titled by "Augmentation of turbulent viscosity", is adopted, which is derived from Lopez de Bertodano *et al.* [10]. They modeled the bubbly two-phase flow turbulence in single liquid phase, the assumption is that the shear-induced turbulence and the bubble-induced turbulence are weakly coupled, therefore can be superposed linearly. This approximation is expected to most valid for dilute bubbly flows. Thus, the Reynolds stress tensor for the continuous phase may be written as:

$$\tau = \tau_1 + \tau_2 \tag{7}$$

where τ_1 is the shear-induced turbulence; τ_2 the bubble-induced turbulence.

From τ_1, the shear-induced turbulence viscosity μ_{t1} is represented by equation (8), which namely the standard model.

$$\mu_{t1} = C_\mu \rho_1 k^2/\varepsilon \tag{8}$$

And they also got the bubble-induced turbulence viscosity μ_{t2} from τ_2 by theoretical analysis as follows:

$$\mu_{t2} = C_3 d_B \alpha_2 U_{slip} \tag{9}$$

where U_{slip} is the absolute value of the slip velocity, C_3 is an empirical constant, as 0.6 [10].

So the total turbulence viscosity gives

$$\mu_t = C_\mu \rho_1 k^2/\varepsilon + C_3 d_B \alpha_2 U_{slip} \tag{10}$$

Compared with equation (8), the turbulent viscosity is augmented by the term of $C_3 d_B \alpha_2 U_{slip}$, so this method is therefore titled by "Augmentation of turbulent viscosity".

(2) Inter-phase drag forces F_i.

The inter-phase drag force has been well noticed in the studies about the bubble driven liquid flow [1–4]. The momentum exchange between the phase can be expressed in terms of these forces acting at the interface between the phases.

The drag force per unit volume is given by:

$$F_{Di} = \left[C_D \frac{\rho_1}{2} A_B (U_{2i} - U_{1i})|U_{2i} - U_{1i}|\right]\frac{n_B}{V_{cell}} =$$

$$\left[C_D \frac{\rho_1}{2}\left(\frac{\pi}{4} d_B^2\right)(U_{2i} - U_{1i})|U_{2i} - U_{1i}|\right]\frac{V_{cell}\alpha_2/\left(\frac{\pi}{6} d_B^3\right)}{V_{cell}},$$

which gives

$$F_{Di} = \frac{3}{4} C_D \frac{\rho_1 \alpha_2}{d_B}(U_{2i} - U_{1i})|U_{2i} - U_{1i}| \tag{11}$$

where C_D is the drag coefficient; A_B the bubble-projected area; V_{cell} the cell volume; d_B the bubble diameter.

The drag coefficient C_D can be expressed as a function of the Eötvös number [4]:

$$C_D = \frac{0.622}{\frac{1}{Eo_B} + 0.235} \qquad 500 < Re_B < 5\,000 \tag{12}$$

where $Eo_B = g d_B^2 \rho_1/\sigma$, is the Eötvös number of the bubbles, $Re_B = d_B U_{slip}\mu/\rho_1$ is the Reynolds number of the bubbles.

2.3 Boundary conditions

(1) Symmetric condition.

At the axis, *i.e.*, the centerline, a no-flux condition (zero normal gradients of flow variables) is imposed at the axis:

$$\frac{\partial U_x}{\partial x} = \frac{\partial U_z}{\partial y} = \frac{\partial \alpha}{\partial x} = \frac{\partial k}{\partial x} = \frac{\partial \varepsilon}{\partial y} = 0 \tag{13}$$

$$U_x = U_y = 0 \tag{14}$$

(2) Wall function.

At the walls, all velocities are set to zero, *i.e.*

$$U_x = U_y = U_z = 0 \tag{15}$$

However, in order to preclude the solution of the governing equations right to solid boundaries where steep gradients of flow variables occur, a log-law wall function is employed to deduce k and ε, wall shear stress and velocity components parallel to the boundary at the first computational grid point adjacent to this boundary [11].

(3) Free surface condition and outlet condition.

The free surface is assumed to be flat, frictionless and impervious to liquid. However, gas is allowed to leave by the rate at which it arrives at the surface, the velocity gradient for existing gas can be regarded as zero. The zero gradient boundary conditions for k and ε are introduced at the top. The pressure is fixed to atmosphere such that the velocities are calculated from the need to satisfy mass conservation at the computational cell adjacent to the surface. These conditions are expressed mathematically as follows:

$$\frac{\partial U_{1x}}{\partial z} = \frac{\partial U_{1y}}{\partial z} = \frac{\partial k}{\partial z} = \frac{\partial \varepsilon}{\partial z} = \frac{\partial U_{2z}}{\partial z} = \frac{\partial \alpha_2}{\partial z} = 0 \tag{16}$$

(4) Inlet conditions.

At the center of the ladle bottom the inlet of gas exists. Flat velocity profiles are assumed for the gas at the orifice exit, *i.e.*, only a vertical gas velocity exists at the inlet nozzle. The liquid volume fraction is considered to be negligible at the nozzle exit, *i.e.*

$$U_{1x} = U_{1y} = U_{1z} = U_{2x} = U_{2y} = 0 \tag{17}$$

$$\alpha_1 = 0.0, \quad \alpha_2 = 1.0 \tag{18}$$

$$U_2 z = U_o = \frac{4Q}{\pi d_o^2} \tag{19}$$

where Q is the gas flow rate; d_o is the nozzle diameter.

The turbulence parameters at the inlet quotes that of O. J. Ilegbusi *et al.* [12] as follows:

$$k=0.015U_o^2 \tag{20}$$

$$\varepsilon=\frac{94k^{1.5}}{d_o} \tag{21}$$

3 Results and discussion

3.1 The fluid flow behavior under the experiment conditions

Figure 2 shows the relationship between the gas holdup at the centerline $\alpha_{2,cl}$ and the height z. When gas

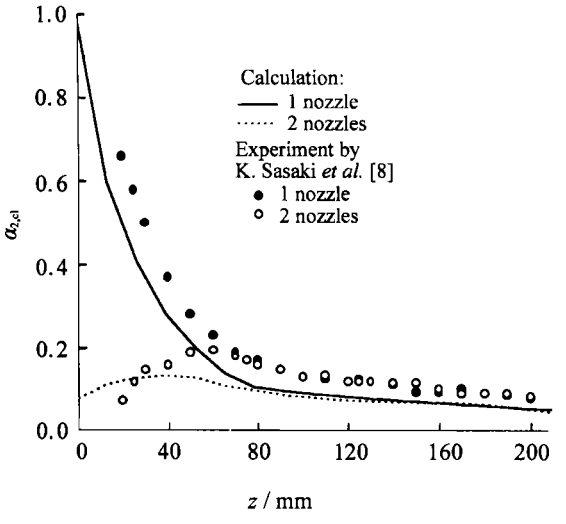

Figure 2 The gas holdup distribution along the centerline of the vessel.

injection is by one nozzle, the gas holdup decreases with z all the time, but when by two nozzles, the gas holdup firstly increases, after one peak value, it decreases again. According to the experiment [8], for the case with two nozzles, the two jets intersect each other when $z>6.2L_H$, *i.e.*, >120 mm in this case. From figure 2, it can be seen, both the experiment and the calculation show that after z >120 mm, the gas holdup distribution with one gas jet is the same as that with two gas jets. Good agreement exists between calculation and experiment.

Figure 3 shows the gas holdup distribution along radical direction at z =150 mm. The gas holdup profiles is approximately bell-shaped, with the maximum values along the axis of the vessel. Almost the same distributions are seen for the case of with one nozzle and that with two nozzles, which means that the movement of bubbles is identical after z >120 mm for the two cases.

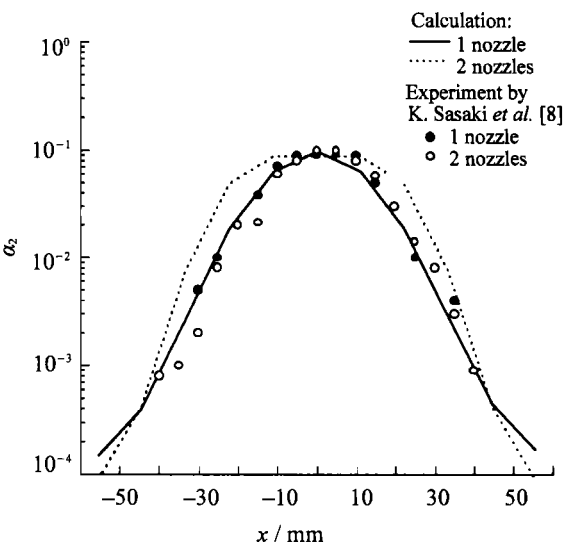

Figure 3 The gas holdup distribution along the radical direction at z = 150 mm.

Figure 4 is the change of the axial liquid velocity with z, the tendency is similar with that of gas holdup distribution. For z >120 mm, the velocities for the case of injection with one nozzle are the same as that with two nozzles. It is well known that for this kind of two phases flow, the liquid flow is generated by the bubble movement, as previous discussion, the bubble movement is identical, so the liquid flow characteristics are also identical.

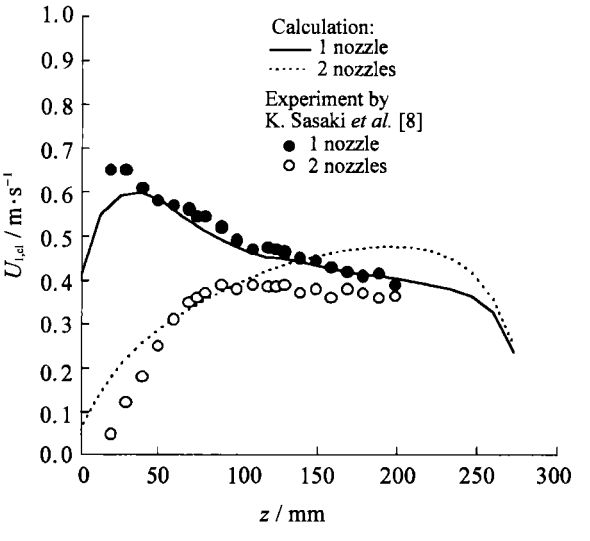

Figure 4 The axial liquid velocity distribution along the centerline of the vessel.

The axial liquid velocities along radical direction at z =150 mm are showed in **figure 5**, which also indicate the same distributions for the cases with one or two nozzles.

Consequently, for the objected vessels, under the condition of L_H = 20 mm, the liquid flow behavior for the case with two gas jets injection is the same as that

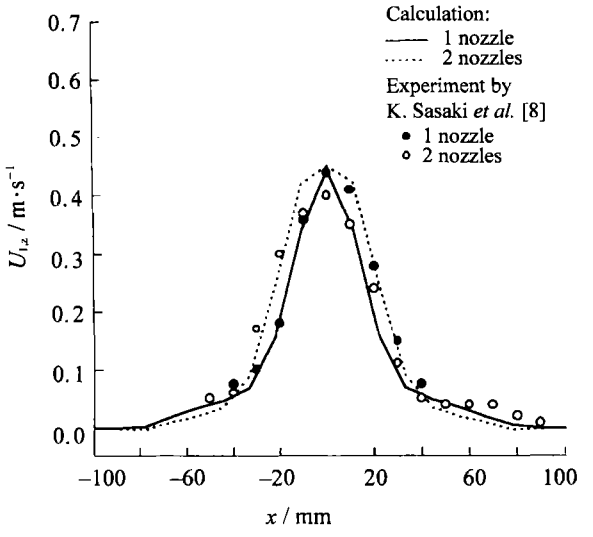

Figure 5 The axial liquid velocity distribution along the radical direction at z = 150 mm.

with one nozzle for z>120 mm. But when using two nozzles, because the gas-liquid interface is bigger than that with one nozzle, so it is favorable for improving the chemical reaction between gas and liquid, then is a better choice for some metallurgical processing.

From figure 2 to figure 5, it is clearly seen that the calculated results agree well with the measured ones, which means this two-phase model is suitable for simulating the fluid behavior of this objected systems, it also indicates that the new-introduced turbulent viscosity model (equation (10)) is right. It is feasible to use this model to predict the fluid flow under related conditions.

3.2 The effect of the distance of two nozzles on the fluid flow

It is easily to imagine that if we change the distance of the two nozzles, *i.e.*, L_H in figure 1, the fluid flow behavior will be changed. That means that this distance has effect on the fluid flow. **Figure 6** is the calculated

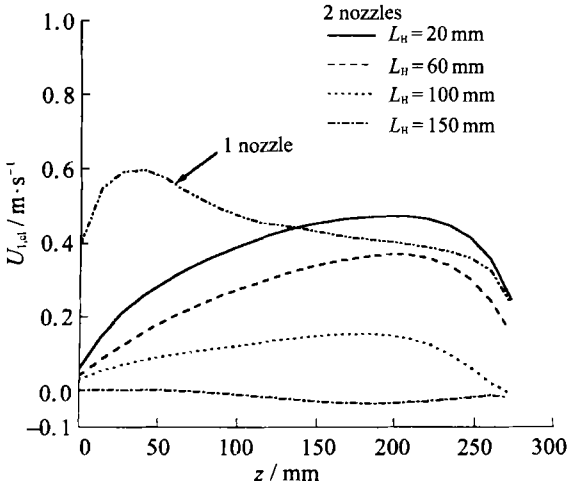

Figure 6 The axial liquid velocity distribution along the centerline under the condition of different L_H.

axial velocity distributions along the centerline of the vessel with different L_H. It is obvious that with the increasing of L_H, the velocity is decreased at the same radical position. When L_H=150 mm, the axial liquid velocities along the centerline are almost zero. If L_H >60 mm, there is no intersection between the curve with one nozzle gas injection and that with two nozzles, which means the fluid flow behavior is different if the distance of the two nozzles is changed.

Figures 7 and **8** show the gas holdup and axial velocity distributions along radical direction at different z under the condition of different L_H. It is easily seen that

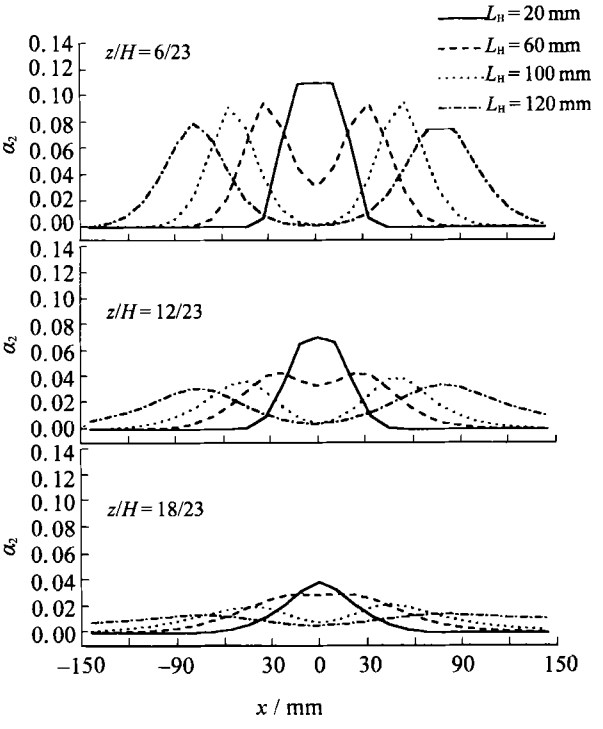

Figure 7 The Calculated gas holdup distribution along radical direction at different z under the condition of different L_H.

the fluid flow characteristics are not identical. For the case of L_H = 20 mm, there is only one peak, but for the other three cases (L_H = 60, 100 and 150 mm), there are two peaks. The two peaks' distance becomes bigger with the increasing value of L_H. The peak values of the four conditions are almost same at the height of z/H= 6/23, but the differences between the peaks of the four cases become big with the increasing of z, and the peaks value of the case with L_H = 20 mm is the biggest.

Figure 9 is the relationship between the calculated mean turbulent energy dissipation rate $\bar{\varepsilon}$ and the value of L_H for the objected systems. It should be mentioned that the center of L_H coincides with the bottom center of the vessel. In this figure, the black points are calculated values, and the line curve is regressed from these values, the regressed equation is:

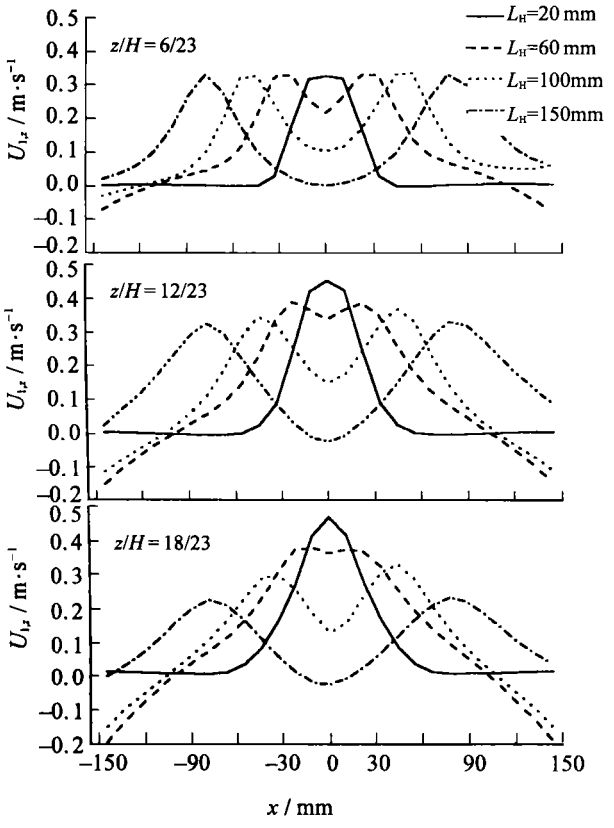

Figure 8 The Calculated axial velocity distribution along radical direction at different z under the condition of different L_H.

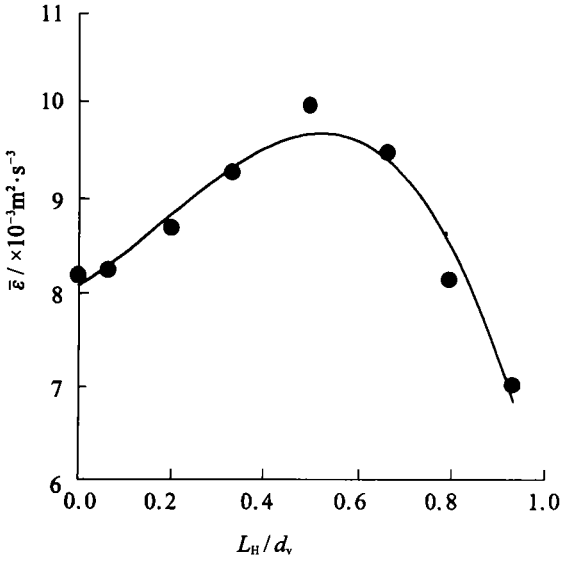

Figure 9 The relationship between the mean stirring intensity and the value of L_H.

$$1\,000\bar{\varepsilon} = 8.09 + 2.95\,(L_H/d_v) + 6.50\,(L_H/d_v)^2 - 11.91\,(L_H/d_v)^3 \quad (22)$$

It is easily seen that when L_H/D is about 0.5, $\bar{\varepsilon}$ is maximum, which means the two gas injection nozzles are located at the 1/4 and 3/4 places of the bottom diameter. It is well known that stirring intensity, *i.e.*, the turbulent energy dissipation rate ε, has a vital effect on the mixing condition, *i.e.*, the bigger value of ε generates better mixing rate. Consequently, when the water in a cylindrical vessel is stirred by two gas jets from the bottom, the best positions of the two nozzles to get a best mixing are the 1/4 and 3/4 places of the bottom diameter.

3.3 The calculated result of practical ladle systems

A comprehensive study of hydrodynamics in full-scale liquid metal processing ladles poses serious experimental difficulties. It is therefore useful to extrapolate the present mathematical model beyond its currently validated limits of vessel size, gas flow rate, and liquid, to predict plume velocities, average recirculation speeds, and liquid steel flow and turbulence energy field, in industrial vessels.

As an example of the model's capabilities in this respect, the fluid flow fields of an 80 t ladle are predicted in **figure 10**. This ladle is with a bottom diameter of 2.0 m, an upper diameter of 2.5 m and a height of 2.8 m.

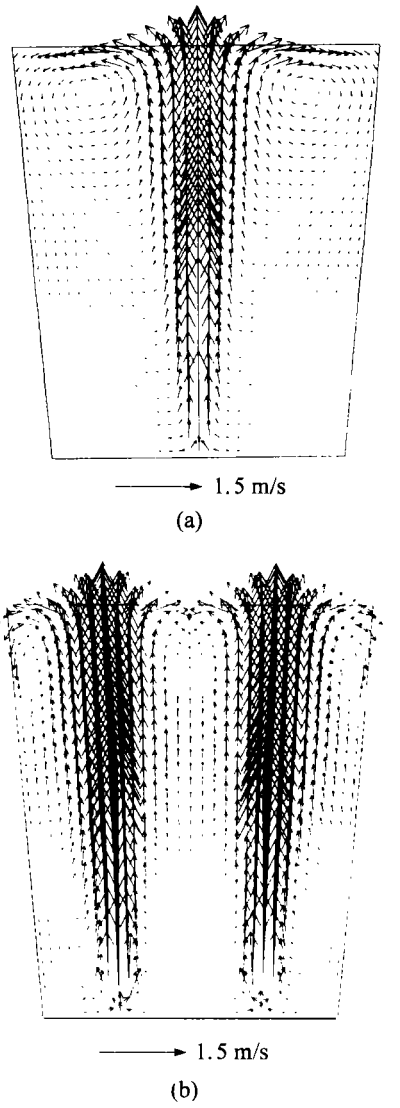

Figure 10 The fluid flow velocity vectors at the main vertical plane of 80 t ladle, (a) gas injection by one nozzle; (b) gas injection by two nozzles.

The total gas flow rate is 3.0×10^{-3} m³/s, which means that as for the case of only with one nozzle the gas flow rate of this nozzle is 3.0×10^{-3} m³/s, but as for the case of with two nozzles, the gas flow rate is 1.5×10^{-3} m³/s for every nozzle. The liquid steel parameters are [9]: ρ_{Fe} = 7 000 kg/m³, μ_{Fe} = 0.007 Pa·s, σ_{Fe} = 1.89 N/m.

Figure 10 (a) is the flow pattern for the case of using one gas jet located in the center of the bottom, and Figure 10 (b) is for the case of using two jets placed at the half radii of one diameter. When with one air jet, there are vortexes near the free surface, liquid steel recirculates around the vortexes. When with two gas jets, the liquid movement is almost in upward direction, and has smaller dead zone compared with that with one jet.

Figure 11 shows the turbulent energy dissipation rate distribution at the main vertical plane, it is easily seen that a larger ε value is generated and so that a well mixing is reacted for the case of with two gas jets than with one gas jet.

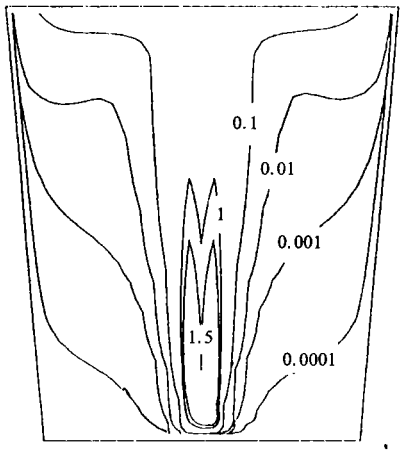

(a)

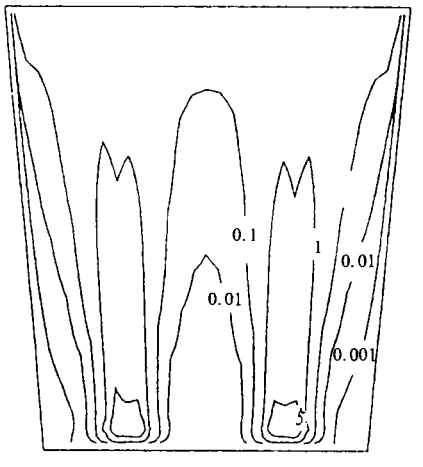

(b)

Figure 11 The turbulent energy dissipation rate (ε) distribution at the main vertical plane of 80 t ladle, (a) gas injection by one nozzle; (b) gas injection by two nozzles, unit: m²/s³.

Figure 12 is the gas plume shape, *i.e.*, the gas holdup isoline of α_2 = 0.01. The gas is better dispersed for the case of with two nozzles than that with one nozzle.

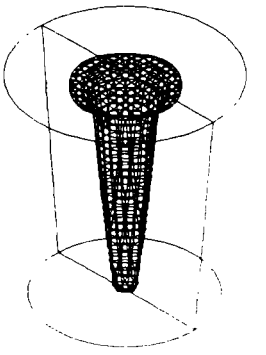

(a)

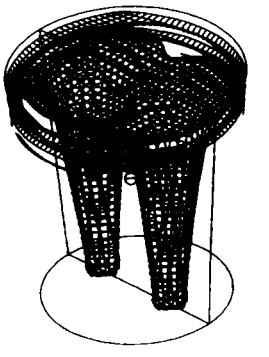

(b)

Figure 12 The gas plume shape,i.e.,the gas holdup isoline of α_2 = 0.01; (a) gas injection by one nozzle; (b) gas injection by two nozzles.

Consequently, in the industrial production, it is useful to use two nozzles to inject gas, by which a much better mixing can be realized than that with one nozzle under the condition of using the same total gas flow rate.

4 Conclusions

(1) Based on a two-phase Eulerian-Eulerian model, the two dimensional fluid flow in air-stirred water systems is simulated. A new turbulence modification model is introduced to consider the bubbles movement contribution to k and ε. The mathematical simulation agrees well with the experiment results. It is feasible to use this model to predict the fluid flow under related conditions.

(2) For the objected vessels, under the condition of L_H = 20 mm, the liquid flow behavior for the case with two gas jets injection is the same as that with one nozzle if z is bigger than 120 mm. Because the gas-liquid interface when using two gas jets is larger than that with one nozzle, which is favorable for improving the

reaction between gas and liquid, it is a better choice to use two gas jets injection for some metallurgical processing.

(3) The distance of two nozzles has big effect on fluid flow behavior in the vessel. When L_H/d_v is about 0.5, the mean stirring intensity is maximum, so it is the best choice to get a best mixing of the bath.

(4) Extrapolating the mathematical model from water system into industrial vessels, the fluid flow of Ar-stirred ladles is calculated. The results indicate that using two gas injection nozzles at the half radii of one diameter of the bottom generates a much better mixing than with one nozzle under the condition of using the same total gas flow rate.

Nomenclature

A_B: bubble projected area, m^2;
C_1: constant, 1.44;
C_2: constant, 1.92;
C_3: constant, 0.6;
C_D: drag coefficient;
C_μ: constant, 0.09;
D: effective phase diffusion coefficient, m^2/s;
d_B: bubble diameter, m;
d_o: nozzle diameter, m;
d_v: vessel diameter, m;
Eo_B: bubble Eotvos number;
F: inter-phase force terms, N/m^3;
F_D: inter-phase drag force, N/m^3;
g: acceleration due to gravity, m/s^2;
G: the production rate of turbulent energy, m^2/s^3;
H: height of the vessel, m;
k: turbulent energy, m^2/s^2;
L_H: the distance of two gas injection nozzles, m;
n_B: bubble number in the volume of V_{cell};
P: pressure, N/m^2;
Q: the gas flow rate, m^3/s;
Re_B: bubble Reynolds number;
S: intra-phase source term, N/m^3;
S^*: inter-phase source term, N/m^3;
U: velocity, m/s;
$U_{l,\,cl}$: the liquid mean velocity at the centerline of the vessel, m/s;
U_o: gas injection velocity at the outlet of nozzle, m/s;
U_{slip}: slip velocity, m/s;
V_{cell}: cell volume, m^3;
α: volume fraction;
$\alpha_{2,\,cl}$: the gas holdup at the centerline of the vessel;
ρ: density, kg/m^3;
ε: turbulent energy dissipation rate, m^2/s^3;
Γ: exchange coefficient;
σ: surface tension;
Pr: turbulent dispersion Prandtl number;
σ_k: constant, 1.0;
σ_ε: constant, 1.3;
ϕ: the name of variable;
μ_l: laminar viscosity;
μ_t: turbulent viscosity;
μ_{eff}: effective viscosity;
τ: Reynolds stress tensor.

Subscript

i: direction, $i = x, y, z$;
m: the type of phases, $m = 1, 2$;
1: liquid phase;
2: gas liquid.

References

[1] O. J. Ilegbusi, J. Szekely: *ISIJ International*, 30 (1990). p. 731.
[2] H. Turkoglu, B. Farouk: *ISIJ International*, 31 (1991). p. 1371.
[3] J. S. Woo, J. Szekely, A. H. Castillejos, J. K. Brimacombe: *Matall. Trans. B.*, 21 (1990). p. 269.
[4] S. T. Johansen, F. Boysan: *Matall. Trans. B.*, 19B (1988). p. 755.
[5] P. E. Anagbo, J. K. Brimacombe: *Metall. Trans. B.*, 21B (1990). p. 637.
[6] Y. Sahai, G. R. St. Pierre: [In:] *Advances in Transport Processes in Metallurgical Systems*, Elsevier, Amsterdam, New York, 1992. p. 259.
[7] Miao-Yong Zhu, T. Inomoto, I. Sawada, Tse-Chiang Hsiao: *ISIJ International*, 35 (1995). p. 472.
[8] K. Sasaki, M. Iguchi: *Tetsu-to-Hagané*, 85 (1999) p. 6.
[9] Laihua Wang, Hae-Geon LEE, P. Hayes: *ISIJ International*, 36 (1996). p. 7.
[10] M. Lopez de Bertodano, R. T. Jr. Lahey, O. C. Jones: *Int. J. Multiphase flow*, 20 (1994). p. 805.
[11] B. E. Launder, D. B .Spalding: *Comp. Meth. Appl. Mech. Engg*, 3 (1974). p. 269.
[12] O. J. Ilegbusi, M. Iguchi, K. Nakajima, M. Sano, M. Sakamoto: *Metall. Trans. B.*, 29B (1998). p. 211.